ORIGINAL ARTICLE

Network Neuroscience Reveals Distinct Neuromarkers of Flow During Media Use

Richard Huskey [ID] [1], Shelby Wilcox[1], & René Weber [ID] [2]

1 Cognitive Communication Science Lab, School of Communication, The Ohio State University, Columbus, OH 43210, USA
2 Media Neuroscience Lab, Department of Communication, University of California Santa Barbara, Santa Barbara, CA 93106, USA

Flow is characterized by a high level of intrinsic reward that results from a balance between task difficulty and individual ability. The Synchronization Theory of Flow offers an explanation for the neural basis of this process. It predicts an energetically-optimized, brain-network organization between cognitive control and reward regions when task difficulty and individual ability are balanced. While initial results provide support for structural predictions, the many-to-many connectivity and energetic optimality hypotheses remain untested. Our study addresses this gap. Subjects played a video game while undergoing functional magnetic resonance imaging. We experimentally manipulated task difficulty and individual ability. Using graph theoretical analyses, we show that the balanced-difficulty condition (compared to low- or high-difficulty) was associated with the highest average network degree in the fronto-parietal control network (implicated in cognitive control) and had the lowest global efficiency value, indicating low metabolic cost, and thereby testing Synchronization Theory's core predictions.

Communication scientists have long concerned themselves with potential, negative consequences associated with media use. Less studied are potentially positive outcomes (Reinecke & Oliver, 2017). Increasingly, however, communication scientists have broadened their scope to include self-transcendent media experiences that uplift and inspire audiences (Oliver et al., 2018). One of the more developed components of this research agenda investigates the state of flow (Csikszentmihalyi, 1990) during media use (Kryston, Novotny, Schmälzle, & Tamborini, 2018; Sherry, 2004).

Corresponding author: Richard Huskey; e-mail: huskey.29@osu.edu; [ID] orcid.org/0000-0002-4559-2439

Csikszentmihalyi (1990) defined the term "flow" to describe a state of optimal experience through total engagement and absorption that is observable in a variety of everyday experiences. The flow state is experienced as highly pleasurable and intrinsically rewarding. Therefore, individuals seek out experiences that will result in flow (Nakamura & Csikszentmihalyi, 2005). Media use is one source of the flow state. Indeed, media use is often described as highly enjoyable, and the psychological process of flow has been offered as an explanation for both media selection and enjoyment (Sherry, 2004).

The flow state depends on characteristics of both the media stimulus and the individual. Three specific antecedents are required in order to experience flow. The flow-inducing stimulus must feature clear goals, with distinguishable rules; a balance between high levels of task difficulty and individual ability; and immediate performance feedback (Nakamura & Csikszentmihalyi, 2005). For Csikszentmihalyi (1975, pp. 36–37) "games are obvious flow activities, and play is the flow experience par excellence." Accordingly, when the antecedents of flow are met (such as when playing an interactive video game), the accompanying experience is characterized by: (a) a state of intense concentration on the task, (b) diminished self-consciousness, (c) a merging of action and awareness, (d) a strong sense of control over the situation, (e) a loss of temporal awareness, and (f) a high level of intrinsic reward, where the task itself is perceived as motivationally relevant.

Empirical evidence generally supports these conclusions. For instance, experimental research shows that a balance between task difficulty and individual ability is associated with the highest level of intrinsic reward during video game play (Keller & Bless, 2008), and the extent to which an individual experiences flow while playing a video game shapes subsequent media effects (Matthews, 2015). Moreover, the flow state is positively correlated with an intention to use media (Liu, Liao, & Pratt, 2008). Research also shows that some individuals are more likely to experience flow than others. Individuals with high levels of intrinsic motivation—that is, people with an autotelic personality—are more likely to experience flow in the first place (Keller & Blomann, 2008; Ross & Keiser, 2014). In fact, this autotelic personality appears to have distinct neurobiological (Gyurkovics et al., 2016; de Manzano et al., 2013) and genetic underpinnings (Mosing, Magnusson, et al., 2012; Mosing, Pedersen, et al., 2012; Wichers et al., 2008).

While we increasingly know the ways in which media content interact with individual differences to result in flow, the neuropsychological underpinnings of this process are less clear. A recent article in *Communication Theory* provides an explanation for these processes (Weber, Tamborini, Westcott-Baker, & Kantor, 2009); however, communication scientists have just begun to test the core neuropsychological premises of the theory (Weber, Huskey, & Craighead, 2017). Accordingly, many questions remain unanswered. This paper tests two theoretically-derived predictions about the neural basis of flow. The first examines the brain-network connectivity associated with flow during media use. The second investigates the energetic costs of network-synchronization processes during flow.

We begin by describing the Synchronization Theory of Flow during media use (Weber et al., 2009; Weber, Huskey, & Craighead, 2017) and the findings to date that support the theory's hypotheses. Next, we lay out brain network fundamentals and explain why more sophisticated analyses are required to test Synchronization Theory's main predictions. Finally, we discuss what communication scientists gain by studying the neural processes underlying flow during media use, including the implications of these results for Synchronization Theory specifically and communication research more generally.

The neural basis of flow

Recent theory building has focused on characterizing the neural basis of flow during media use. Specifically, the Synchronization Theory of Flow (Weber et al., 2009; Weber, Huskey, & Craighead, 2017) outlines a framework that puts the concept of flow on a communication neuroscience foundation (see Weber, Fisher, Hopp, & Lonergan, 2017; Weber, Sherry, & Mathiak, 2008). Synchronization Theory posits that flow results from the synchronization (also known as functional connectivity) between distinct brain networks when task difficulty is matched with individual ability. From this central premise, Synchronization Theory outlines four key hypotheses.

> H1: Flow results in a network synchronization process between cognitive control and reward networks.
> H2: Network synchronization during flow is a discrete state that is separable from other neuropsychological states.
> H3: Network synchronization corresponds to an energetically-optimized brain state.
> H4: Network synchronization manifests as an enjoyable experience.

Nearly a decade has passed since Synchronization Theory was first introduced, and evidence in support of its central hypotheses is beginning to accumulate. For instance, the neural correlates associated with flow during media use show that flow requires neural activity in cognitive control and reward networks (Klasen, Weber, Kircher, Mathiak, & Mathiak, 2012; Ulrich, Keller, & Grön, 2016a, 2016b; Ulrich, Keller, Hoenig, Waller, & Grön, 2013). Our own research takes this one step further, by testing the synchronization (or functional connectivity) patterns between these structures. Our results provide support for the claim that, when task difficulty is balanced with individual ability, a network synchronization process occurs between cognitive control and reward networks, and this results in an intrinsically-rewarding flow state (Huskey, Craighead, Miller, & Weber, 2018). Taken together, this preliminary evidence provides empirical support for H1.

Still, questions remain. The first is dependent on a technical detail about the way in which the "synchrony" hypothesis (H1) was tested by Huskey et al. (2018). Specifically, it relied on psychophysiological interaction analyses (PPI; Friston et al.,

1997; Huskey, 2016), a method where neural activity in just one brain region shows a statistical dependency with all other regions in the brain. The PPI analysis employed by Huskey et al. (2018) showed that the nucleus accumbens (a key structure in the reward network) was functionally connected with key regions in the frontoparital control network, including the dorsolateral prefrontal cortex and paracingulate gyrus. However, the PPI approach is limited, in that it only shows how one brain region (in this case, the nucleus accumbens) is connected to several other brain regions. Importantly, such a one-to-many approach to studying brain networks necessarily oversimplifies the true network topology of the brain during flow, where multiple regions should be simultaneously, functionally connected. Said differently, an analysis is needed that evaluates how each member of a network is simultaneously, functionally connected with all other members of the network. Therefore, a more sophisticated treatment that allows for studying the many-to-many network architecture of the brain is needed to better test the network connectivity hypothesis (H1). A second issue is that classic, analytical paradigms for evaluating brain activity during communication processes (such as the general linear model, see e.g., Weber, Mangus, & Huskey, 2015) do not tell us anything about energetic optimality. Accordingly, Synchronization Theory's optimality hypothesis (H3) remains untested. Our present study addresses both of these issues, by using recent advances in network neuroscience to integrate a core understanding of how media content contribute to flow experiences (Bassett & Sporns, 2017; Falk & Bassett, 2017; Turner, Huskey, & Weber, 2018).

Fundamentals of brain networks

The history of functional magnetic resonance imaging (fMRI) research is characterized by a strong focus on spatially localizing cognitive processes (e.g., identifying the neural correlates of communication process Y). So much so, in fact, that this endeavor has its own pejorative term: "blobology" (Poldrack, 2012). However, recent technical, statistical, theoretical, and philosophical advances are pushing the field toward an understanding of the brain—and the cognitive processes it enables—as the result of complex, networked interactions between multiple brain regions (Bassett & Gazzaniga, 2011). One analytical framework for dealing with such networked data, long familiar to many communication scientists (e.g., Monge & Contractor, 2003), is graph theory (for an introduction, see Newman, 2010). Incredible strides have been made over the last few years in outlining both theory (Bassett & Gazzaniga, 2011; Falk & Bassett, 2017; Sporns, 2011, 2012) and method (Fornito, Zalesky, & Bullmore, 2016; Rubinov & Sporns, 2010; Sizemore & Bassett, 2017) for applying graph theory to brain data, such that a field of network neuroscience is rapidly emerging (Bassett & Sporns, 2017).

Treating the brain as a network graph, where nodes in the graph represent brain regions of interest (ROIs) and the edges in the graph represent functional connections between nodes, has tremendous utility for testing Synchronization Theory. At

the most basic level, it allows us to observe the many-to-many connections associated with flow in ways that more traditional approaches (e.g., PPI) do not. Accordingly, and consistent with H1, we should expect the strongest network connectivity patterns (as measured by average network degree) to be between the cognitive control (particularly the fronto-parietal control network) and reward (subcortical) networks during flow.

The second aim of this manuscript is to test Synchronization Theory's energetic-optimality hypothesis (H3). There is considerable evidence that synchronization in both non-biological and biological systems is energetically efficient (Strogatz, 2003), and that this is also true for neural systems (Laufs et al., 2003). This principle has been offered as an explanation for why flow is perceived as not physically or mentally taxing, even though flow-inducing tasks require a high level of difficulty. Importantly, however, we know that different, synchronized brain states have different, energetic costs, and that these energetic costs correspond with task performance. For instance, Bassett et al. (2009) show that a more energetically-efficient brain-network organization is associated with increased performance during a cognitive control task. Said differently, these results "echo the saying that 'less is more': The information processing performance of a network can be enhanced by a sparse or low-cost configuration with disproportionately high efficiency" (Bassett et al., 2009, p. 11747). This is not always true, however, as there is some evidence that less energetically-efficient network organizations improve task performance, at least for auditory discrimination tasks (Weiss et al., 2011). Therefore, if the high levels of difficulty and ability associated with flow engage cognitive control mechanisms, then we should expect a brain network that is organized in an energetically-efficient topology (as characterized by connections between nodes within a network).

Importantly, graph theory offers a number of analytical techniques for characterizing the energetic costs associated with different brain networks. Foundational work in this area shows that different network topologies have different metabolic and information-transfer properties (Bullmore & Sporns, 2012). For instance, a brain where every node is connected to every other node has a high global-efficiency value (Latora & Marchiori, 2001), as information in one node needs to make just one jump to reach any other node. Higher global efficiency allows the brain to quickly encode large amounts of information and efficiently synthesize signals from a number of nodes throughout various brain regions (Davison et al., 2015). However, the key insight of Bullmore and Sporns (2012) is that high levels of global efficiency are metabolically costly when compared to lower levels of global efficiency (where fewer nodes are functionally connected). Accordingly, brain networks dynamically reconfigure based on task demands (Cole et al., 2013; Davison et al., 2015; Gu et al., 2015; Hermundstad et al., 2013), where the brain balances the optimal trade-off between global efficiency and metabolic cost. Therefore, if H3 in Synchronization Theory is correct, then we should expect to see a lower global-efficiency (low metabolic cost) brain-network configuration during flow.

Implications for communication theory

As communication scientists, we aim to understand how moment-by-moment changes in media content contribute to flow experiences. This has both scientific (e.g., Sherry, 2004) and practical implications (e.g., designing messages that boost audience engagement). However, and as others have written about extensively elsewhere (Weber et al., 2009, Weber, Huskey, & Craighead, 2017), the existing methods for measuring flow make this objective all but impossible. State-of-the-art techniques include either (a) using one of at least 13 different self-report measures (Novak, Hoffman, & Yung, 2000) taken at the conclusion of media use, or (b) applying the experience sampling method (ESM; Kueby, Larson, & Csikszentmihalyi, 1996). Beyond concerns about post hoc reflection (Nisbett & Ross, 1980), as well as the large number of different scales that all purport to measure flow, self-report measures collected after media use are not suitable for identifying the specific content features that contribute to flow. In a way, the ESM solves this problem, by stopping subjects at various times during media use to see if they are experiencing flow. Unfortunately, this procedure introduces a new confound, in that it disrupts the flow experience, thereby making it impossible to observe how media dynamics contribute to flow.

Therefore, truly understanding how dynamic changes in media content contribute to flow requires an unobtrusive and online measure. Solving this theoretical puzzle requires methodological innovation (for an extended treatment on theory/method synergy, see Greenwald, 2012). We propose that changes in brain-network characteristics (as measured using graph theoretical techniques) during media use may serve as a neruromarker of flow. If true, then this neuromarker will finally enable communication scientists to study how content dynamics contribute to flow. Our study lays the foundation for this line of inquiry.

Methods

Previous reporting and general overview

This manuscript uses fMRI data previously reported in Huskey et al. (2018). Whereas our earlier analyses on this dataset relied on the classic, general linear model approach for analyzing fMRI data, the present study applies analytical procedures adopted from network neuroscience (Bassett & Sporns, 2017). These new analytical procedures allow us to test a priori–defined hypotheses, as specified by Synchronization Theory. Here, we provide a brief overview of the procedure.

FMRI data acquisition

All data were collected on a Siemens Magnetom Prisma (3-Tesla) fMRI scanner. The blood-oxygen level–dependent contrast was measured using a multiband echo planar gradient sequence (Ugurbil et al., 2013) acquired parallel to the AC-PC plane (TR = 720.0 ms, TE = 37.0 ms, FA = 52 degrees, FOV = 208 mm, multiband acceleration factor = 8). A total of 72 interleaved slices comprised each volume; spatial

resolution was 2 mm^3. A high-resolution T1-weighted sagital sequence was also collected (TR = 2500.0 ms, TE = 2.22 ms, FA = 7, FOV = 241mm, .9 mm^3).

FMRI data preprocessing

Our fMRI data were cleaned following a three-stage pre-processing pipeline (see e.g., Weber et al., 2015) using fMRI Expert Analysis Tool v6.0 from the Oxford Center for Functional MRI of the Brain (FMRIB) Software Library (FSL v5.0). In the first stage, data were brain extracted (BET; Smith, 2002) and spatially aligned (MCFLIRT; Jenkinson, Bannister, Brady, & Smith, 2002). Of note, and following new recommendations, the data were not spatially smoothed (Alakörkkö, Saarimäki, Glerean, Saramäki, & Korhonen, 2017). In the second stage, the data were filtered for motion artifacts using an independent components analysis based procedure (Pruim, Mennes, Buitelaar, & Beckmann, 2015; Pruim, Mennes, van Rooij, et al., 2015). In the final stage, the functional data were high-pass filtered (sigma = 360s), coregistered to the T1 (FLIRT Jenkinson et al., 2002), and registered to the MNI152 standard template using a nonlinear transformation (FNIRT; Andersson, Jenkinson, & Smith, 2007a, 2007b). Detrended timeseries data were then extracted from these filtered functional data (see Defining the Network subsection below).

Subjects and experimental procedure

A total of 18 subjects completed the study (M_{age} = 22.83; female = 77.8%). Subjects were recruited from the University of California Santa Barbara, and all procedures were approved by the University's institutional review board. In this study, subjects completed four experimental runs where they played a well-validated, naturalistic, and open-source, experimental video game (Asteroid Impact; https://github.com/richardhuskey/asteroid_impact). Consistent with flow theory and previous methods for experimentally manipulating flow (Keller & Bless, 2008; Ulrich et al., 2013, 2016a, 2016b), our study manipulated three experimental conditions, each lasting for 120s: low-difficulty (ability > difficulty), high-difficulty (difficulty > ability), and balanced-difficulty (difficulty ≈ ability). In the low-difficulty condition, subjects repeatedly played the first (and easiest) level of the game, whereas in the high-difficulty condition, subjects repeatedly played the game's last (and most difficult) condition. In the balanced-difficulty condition, subjects advanced to each subsequent level at their own pace, based on their own individual ability. Subjects completed a total of four runs, where each run contained all three conditions. The condition order was counterbalanced across all subjects. During each condition, subjects were also required to respond to a visual, secondary-task reaction-time measure (STRT, not reported herein; Lang, Bradley, Park, Shin, & Chung, 2006). This experimental manipulation has been validated in a series of three different studies (Huskey et al., 2018), showing that the balanced-difficulty condition results in the highest level of self-reported flow and longest STRTs (high attentional demand for the primary task; i.e., playing the experimental video game) as compared to the low- and high-difficulty conditions.

Open science practices and reporting accuracy

In addition to the open-source stimulus described above, all the code and raw (de-identified) group-level network graphs necessary to recreate our analyses are available from the Open Science Framework project page (https://osf.io/uf5zw/). We now conceptually describe the analysis. For a more detailed treatment of the mathematical background of this analysis, see the Supplementary Appendix.

Network graph analysis

Defining the network

As a first step, the pre-processed fMRI data were analyzed in Python using the Nilearn toolkit (Abraham et al., 2014). In order to define our network graph, we used the Power et al. (2011) atlas. This atlas defines 264 nodes across 14 different, major brain sub-networks (e.g., fronto-parietal, default mode, subcortical). The next step required us to extract neural timeseries data from each node (within a 5 mm sphere), for each subject, for each condition (Figure 1a). These timeseries data were then correlated (Pearson correlation), which resulted in 213[1] unique 264 × 264 correlation matrices (one correlation matrix for each of the 18 subjects, for each of the 4 runs, for each of the 3 conditions), where each row/column in the matrix represented a given node in the network (Figure 1b). These correlation matrices were then averaged to create three group-level correlation matrices, one belonging to each experimental condition. These group-level correlation matrices were output as a text file for further processing. Group-level covariance matrices were also generated using the procedure described above (see Null Network Construction subsection, below). Henceforth, and following network science conventions, these group-level correlation and covariance matrices are referred to as adjacency matrices.

Network processing

The group-level adjacency matrices were then imported to Matlab (version R2017a) for further processing using the Brain Connectivity Toolbox (Rubinov & Sporns, 2010) and Graph-Theoretical Analysis Toolbox (Hosseini, Hoeft, & Kesler, 2012). Following standard processing procedures for brain-network analyses (Fornito et al., 2016), the adjacency matrix for each condition was proportionally thresholded, such that only the strongest 10% of connections were preserved. Additional thresholds were applied to test the robustness of our global efficiency analysis (see below). These thresholded adjacency matricies were then binarized, such that all values were coded either as 1 (a value that survived thresholding) or as 0 (a value that did not survive thresholding; Figure 1c). This resulted in a sparse graph, on which network metrics (both average degree and global efficiency) were calculated (Figure 1d).

Null network construction

The null or sampling distribution of brain-network adjacency matrices is unknown (Fornito et al., 2016). Accordingly, and following established guidelines in the network neuroscience literature (e.g., Zalesky, Fornito, & Bullmore, 2012), we used the
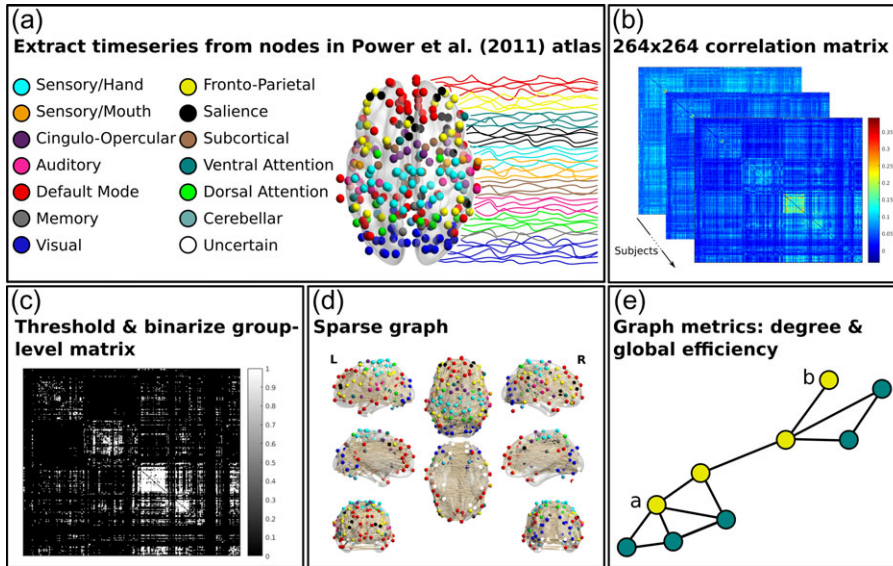
Figure 1 Conceptual schematic of the analysis. (a) We first extracted the neural timeseries data for each node ($n = 264$) in the Power et al. (2011) atlas. This procedure was repeated for each subject, for each experimental condition. (b) The timeseries data were then organized into a 264×264 Pearson correlation matrix for each subject, for each condition. These correlation matrices were averaged to create a group-level adjacency matrix for each condition. (c) Each group-level adjacency matrix was then thresholded and binarized. (d) This resulted in a sparse graph for each condition, on which network (both average degree and global efficiency) metrics were calculated. (e) Degree is the number of edges connected to a given node in a network. Here, node (a) has a degree of 4 and node (b) has a degree of 1. Global efficiency is the average of the inverse of the shortest path length for all nodes in the network. Here, the shortest path length from node (a) to node (b) is 3. Part d was generated using Brain Net Viewer (Xia, Wang, & He, 2013).

Hirschberger-Qi-Steuer algorithm to simulate the sampling distribution of adjacency matrices (Hirschberger, Qi, & Steuer, 2007).[2] Specifically, the empirically-observed covariance matrix for each condition was used to generate a total of 10^4 null covariance matrices for each experimental condition. Each covariance matrix was then converted to a correlation matrix, henceforth referred to as a null adjacency matrix. Each null adjacency matrix was thresholded and binarized using the procedure described in the Network Processing subsection (above). Network statistics were computed on the resulting distribution of null sparse graphs.

Network statistics: degree and global efficiency
The degree—that is, the number of edges for a given node—was calculated for all nodes in the empirical and null sparse graphs. Given that we are interested in the extent to which degree varies by brain network, as identified in the Power 264 atlas (e.g., fronto-parietal control network, subcortical network), we then summed the

total degree for each node in a given network. Since each network contains a different number of nodes (e.g., the fronto-parietal control network contains more nodes than the subcortical network), the average degree for each network was calculated to allow for more interpretable comparisons. For the main analysis, and within each network, we tested whether the degrees were different between the three task conditions. Next, global efficiency (Latora & Marchiori, 2001) values were calculated for each experimental condition and each of the null adjacency matrices. Global efficiency is defined as the average of the inverse of the shortest path length for all nodes in a network[3] (Figure 1e).

Inference testing

We then followed a procedure for calculating paired samples t-tests (two-tailed) from our empirical and randomly-generated network data (for a complete description of the procedure, see Snijders & Borgatti, 1999).[4] With these calculations in place, we were able to test both H1 and H3. Testing H1 relied on looking at the average degree for a given network, which provides information about the many-to-many connections associated with each experimental condition. Specifically, we expected to see the higest average degree between cognitive control (fronto-parietal control) and reward (subcortical) networks in the flow condition. H3, on the other hand, was evaluated based on the global efficiency scores for each experimental condition, and we expected to see the lowest global efficiency score in the flow condition.

Results

Network connectivity patterns

Table 1 shows the average network degree—defined as the average number of edges connected to all nodes in a given network—by experimental condition. Paired-samples t-tests (two-tailed) were used to compare the average degrees within each network, for each of the three task conditions. A false discovery rate (FDR) correction for multiple comparisons was applied to maintain acceptable family-wise error rates.

H1 predicted the highest degree (number of edges between nodes) between cognitive control (fronto-parietal control) and reward (subcortical) networks during the balanced-difficulty condition. This was not observed. Only one node in the subcortical network survived thresholding, and this node showed just one connection, between the right thalamus and visual cortex. Therefore, a strict test of H1 was not supported.

As a more liberal test of H1, we then characterized the average degrees among sub-networks for each condition (Figures 2a–b). If flow does require cognitive control, then we should expect a high average degree among the fronto-parietal control network in the balanced-difficulty condition. The fronto-parietal control, ventral attention, memory, and sensory/mouth networks had the highest average degree in

Table 1 Average Degree of Nodes in Each of the Power et al. (2011) Networks

Network	Total Nodes	Low-Difficulty	Balanced-Difficulty	High-Difficulty
Sensory/Hand	30	9.90	10.03	15.80[‡‡‡]
Sensory/Mouth	5	18.40	24.00[*,‡‡‡]	14.00
Cingulo-Opercular	14	19.36[***]	13.64	24.36[‡‡‡]
Auditory	13	19.62	17.31	23.46[‡‡‡]
Default Mode	58	30.16[***]	20.55	19.45
Memory	5	35.40	41.80[**,‡‡‡]	29.20
Visual	31	57.62	62.61[***]	61.87
Fronto-Parietal	25	35.96	46.68[***,‡‡‡]	35.40
Salience	18	23.39	27.72	33.00[‡‡‡]
Subcortical	13	.23	.00	.08
Ventral Attention	9	22.11	31.33[***,‡‡]	25.44
Dorsal Attention	11	35.09	42.00[***]	49.64[‡‡‡]
Cerebellar	4	2.75	4.50	6.75

Note: Paired-sample *t*-tests (two-tailed) were used to evaluate mean differences for the balanced-difficulty>low-difficulty and balanced-difficulty>high-difficulty pairwise comparisons. The resulting *p*-values were false-discovery-rate corrected using the mafdr function in Matlab to control family-wise error rates. Balanced-difficulty>low-difficulty: *$q < .05$, **$q < .01$, ***$q < .001$.
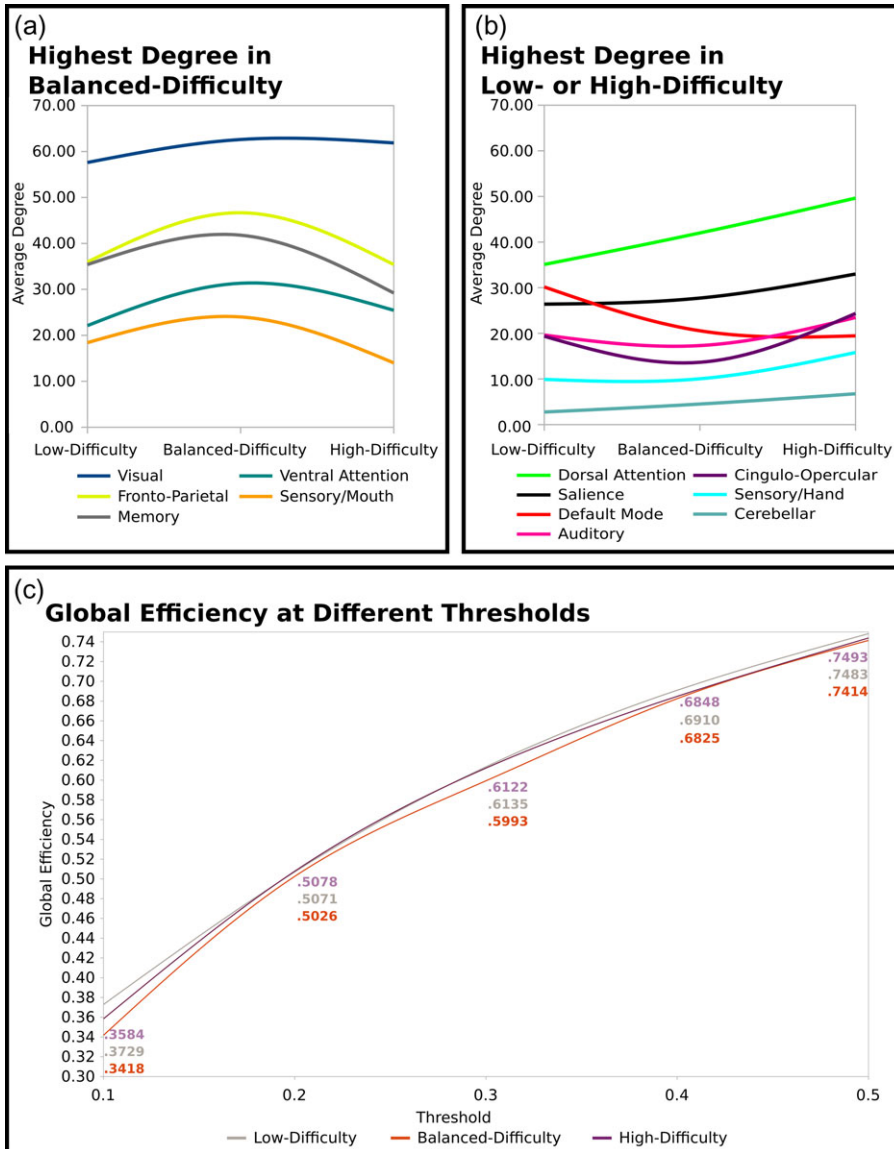Balanced-difficulty>high-difficulty: ‡‡$q < .01$, ‡‡‡$q < .001$.

the balanced-difficulty condition, as compared to the low- or high-difficulty conditions (FDR corrected, all $q < .05$). By comparison, the low-difficulty condition was much more densely connected within the default mode network and the cingulo-opercular network, as compared to the balanced-difficulty condition (FDR corrected, all $q < .001$). Finally, the dorsal attention, salience, sensory/hand, auditory, and cingulo-opercular networks had the highest average degrees in the high-difficulty condition, as compared to the balanced-difficulty condition (FDR corrected, all $q < .001$). It is worth noting that subcortical structures had low average degrees across all conditions, an unexpected result that we consider in detail in the Discussion section.

Global efficiency

H3 predicted that the balanced-difficulty (or flow) condition would have the lowest energetic cost, as reflected by the lowest global efficiency score. To test this, global efficiency scores were calculated for the thresholded network graphs for each experimental condition. The balanced-difficulty condition had the lowest global efficiency score ($E = .3418$), followed by the high-difficulty ($E = .3584$) and low-difficulty ($E = .3729$) conditions.

Paired-samples *t*-tests (two-tailed), following the bootstrapping procedure described above, show a significant difference in global efficiency between the balanced- and high-difficulty conditions ($t = -10.0259$, $p < .00001$). A significant

Figure 2 (a) Sub-networks with the highest average degree in the balanced-difficulty and (b) low- or high-difficulty conditions. (c) The balanced-difficulty condition has the lowest global efficiency values (and therefore is most energetically efficient) across different network thresholds. All pairwise comparisons (two-tailed paired-samples t-tests) were significant at a Bonferroni corrected value of $p < .01$.

difference was also observed between the balanced-difficulty and low-difficulty conditions ($t = -19.1200$, $p < .00001$). There is some evidence that global efficiency values might change depending on the network threshold. To test this, we conducted

this analysis on several different thresholds, and observed consistent results (Figure 2c). Taken together, these results provide support for H3, in that the balanced-difficulty condition was the most energetically-efficient condition.

Discussion

In this study, subjects played a video game where three experimental conditions were manipulated: low-difficulty, balanced-difficulty, and high-difficulty. These conditions were derived from flow theory and have been previously shown to manipulate self-reported flow, attentional demand, and brain network connectivity (Huskey et al., 2018). In the present study, we used a graph-theoretical perspective with two key goals: (a) to test the many-to-many brain-network organization, which is associated with flow experiences during media use (Syncronization Theory H1), and (b) to provide a first-ever test of the Synchronization Theory of Flow's efficiency hypothesis (Synchronization Theory H3). We now turn our attention to each of these findings, before considering their broader implications.

Network connectivity patterns

While our network degree results do not provide support for a strict test of H1, they do replicate previous research in implicating cognitive control as a core component of flow. They also extend our understanding of the network topology underpinning flow. Specifically, we show that the fronto-parietal control network (a key cognitive control network) has the highest average degree in the balanced-difficulty condition, as compared to the low- or high-difficulty conditions. Further, our results are consistent both with a number of previous studies that demonstrated that flow experiences require neural activity in cognitive control networks (Klasen et al., 2012; Ulrich et al., 2013, 2016b) and our own research, which uses PPI analyses and shows that the dorsolateral prefrontal cortex (a structure in the fronto-parietal control network) is connected to a number of core cognitive control structures during flow experiences (Huskey et al., 2018). However, the lack of connectivity among subcortical reward structures, in general, is inconsistent with Synchronization Theory H1 and with our previous findings using PPI analyses. We expand on each of these implications below.

Recent meta-analytic evidence shows that the frontro-parietial control network can actually be split into two sub-systems: one that is connected with the default mode network (DMN; a network that is activated during rest or during highly automatic tasks; see below) and one that shows strong connections with the dorsal attention network (Dixon et al., 2018). This second sub-system is implicated in the regulation of perceptual attention during cognitive control. In our study, the ventral attention network had the highest average degree during the balanced-difficulty condition. The ventral attention network is typically associated with object and motion perception, whereas the dorsal attention network is more commonly implicated in sensorimotor action (Goodale & Milner, 1992). With these distinctions in

mind, and given that the state of flow is characterized by a merging of action and awareness (Csikszentmihalyi, 1990), we might expect a higher average network degree in the dorsal attention network during flow. Therefore, it is somewhat surprising that the average degree for the dorsal attention network was highest in the high-difficulty condition (compared to the low- and balanced-difficulty conditions), although it is worth noting that the average degree in the balanced-difficulty condition was significantly higher than in the low-difficulty condition. One possible explanation for this is that subjects may have deployed more sensorimotor control in the high-difficulty condition in order to meet the elevated task demands. Previous research shows that high levels of distraction from a primary task are associated with decreased connectivity among fronto-control structures, but increased connectivity among sensorimotor structures (Weber, Alicea, Huskey, & Mathiak, 2018). That the hand-motor network also had the highest average degree in the high-difficulty condition but lowest average degree in the fronto-parietal network supports this interpretation.

Interestingly, a recent synthesis suggests that the ventral attention network is sensitive to spatial visual encoding and top-down control, while the dorsal attention network encodes the visual cues involved with more perfunctory actions (Gilaie-Dotan, 2016). With this in mind, the higher average degree in the ventral attention network during the balanced-difficulty condition (compared to the low- and high-difficulty conditions) may suggest that being in the state of flow increases the integration of visual cues and action control, but with lower demands on the dorsal attention network. This may result from a lower local efficiency score (a measure of efficiency within a subgraph of the total network), which should be associated with lower metabolic costs (see Global Efficiency section below). Clarifying this issue requires that future studies focus on better understanding local connectivity between the fronto-parietal control network and the dorsal and ventral attention networks during flow.

Of surprising note, however, is that we did not see strong connectivity patterns between subcortical reward structures and fronto-parietal control structures (as predicted by Synchronization Theory and shown in our own previous research). For the balanced-difficulty condition, only one connection survived thresholding, and this connection was between the right thalamus and a node in the visual cortex. That the thalamus is implicated in flow is consistent with previous research (Klasen et al., 2012; de Manzano et al., 2013; Ulrich et al., 2013), but the lack of connectivity with other subcortical structures is inconsistent with our own previous findings (Huskey et al., 2018). Several possible explanations are available. First, our own previous research has shown that the thalamus is not strongly connected with other brain structures during flow (Huskey et al., 2018). This same study showed that it was, in fact, the nucleus accumbens (ventral striatum) that was broadly connected to cognitive control regions. However, the subcortical ROIs in the Power 264 atlas (Power et al., 2011) do not include any structures within the ventral striatum, as verified by entering atlas coordinates into Neurosynth (Yarkoni, Poldrack, Nichols,

Van Essen, & Wager, 2011). Accordingly, it seems that our choice of atlas was sub-optimal for testing this hypothesis. Future studies may benefit from augmenting the Power atlas with additional subcortical ROIs. A final explanation is related to a technical aspect associated with the fMRI sequence used in this study. A recent paper shows that multiband sequences with high acceleration factors (e.g., acceleration factor = 8) decrease sensitivity in subcortical structures (Risk, Kociuba, & Rowe, 2018). The present study applied an acceleration factor of 8, which may also explain why so few subcortical connections survived thresholding.

Finally, it is worth noting that the DMN had the highest average degree in the low-difficulty condition. Indeed, a number of previous studies have shown that this network is commonly implicated when there is a mismatch between task difficulty and individual ability (Huskey et al., 2018; Ulrich et al., 2013, 2016a, 2016b). Further still, a growing body of research shows that the default mode network is activated in task-positive conditions associated with boredom (Mathiak, Klasen, Zvyagintsev, Weber, & Mathiak, 2013) and just-published results show strong activity and network connectivity in the DMN when a task has been sufficiently learned, is highly predictable, and therefore can be accomplished on "autopilot" (Vatansever, Menon, & Stamatakis, 2017). Our results corroborate these findings.

Global efficiency

The second aim of our manuscript was to provide a first-ever test of the Synchronization Theory of Flow's energetic-optimization hypothesis. Here, we show that our balanced-difficulty condition has the lowest global efficiency score, and that this is significantly different from the score observed in the low- and high-difficulty conditions. This finding supports Synchronization Theory H3. Accordingly, we now consider what we know about the energetic costs of the brain at rest (DMN) and the brain during flow, which requires cognitive control.

The DMN is typically characterized as the brain at rest (Raichle et al., 2001) or during automatic task processing (Vatansever et al., 2017). The DMN is also characterized by high levels of global brain connectivity, and this dense connectivity is thought to facilitate shifting the brain in and out of a number of different network topologies, corresponding to different cognitive states (Gu et al., 2015). Evidence shows that the DMN is not necessarily metabolically efficient, but its relatively high level of global efficiency may facilitate shifts into network typologies that have lower global efficiency values, thereby enabling metabolically-efficient processing during tasks (Davison et al., 2015).

At the same time, we also know that the cognitive control network is densely connected (Cole, Pathak, & Schneider, 2010; Cole, Yarkoni, Repovs, Anticevic, & Braver, 2012) and that efficient network topologies in fronto-parietal structures are associated with increased task performance (Bassett et al., 2009). Interestingly, there are conflicting results about the relationship between network cost and task performance, with some evidence suggesting that low global efficiency is associated with increased performance (Bassett et al., 2009), whereas other studies show the

opposite relationship (Weiss et al., 2011). This difference in relationship has been attributed to learning processes, differences in task demands, or differences in which brain networks are engaged in the task. Ultimately, these studies show that successfully deploying cognitive control requires an energetically-efficient brain state. Given that flow requires high levels of cognitive control, and that we observed the most energetically-efficient network configuration in the balanced-difficulty condition, we interpret this as strong evidence in support of Synchronization Theory H3.

Media use, flow, and the brain

Back in 2004, Sherry made the case that dynamic changes in media content may alter the balance between task-difficulty and individual ability, thereby shifting media users in and out of flow. After nearly 15 years, many of Sherry's most exciting ideas remain untested. Why? One possible explanation is that communication scientists lack a suitable measure for linking content features with flow. Typically, flow during media use is measured either by self-reports taken after an experimental condition (e.g., Huskey et al., 2018; Keller & Bless, 2008; Ulrich et al., 2016a, 2016b; Ulrich et al., 2013) or by using the ESM (Kueby et al., 1996) to periodically disrupt media use to see whether a particular content feature resulted in flow (e.g., Chen, 2006). Frustratingly, if flow is a state where individuals experience diminished temporal- and self-awareness, then the first approach is not well suited for identifying the specific content features that contributed to flow. To some degree, the second approach resolves this issue, but by introducing a new concern. The ESM disrupts flow, thereby making it impossible to uncover the content dynamics that contribute to flow.

Our study points to a solution, in that we identify two potential neuromarkers of flow: average degree within the fronto-parietal control network and global efficiency. It is worth noting that we use the word "neuromarker" cautiously, as additional validation work is needed. Our analysis was conducted on group-level data that were treated as a fixed effect, which imposes specific limitations on generalizability to larger populations. Moreover, individual-level prediction (Berkman & Falk, 2013; Falk, Cascio, & Coronel, 2015) is necessary in order to test Synchronization Theory H4 (that these neuromarkers predict enjoyment).

In the present study, we looked at these neuromarkers statically across an entire experimental condition. It should be possible, in principle, to design a study that is optimized for evaluating these metrics dynamically during media use. Indeed, just-published procedures make such an analysis mathematically tractable (Sizemore & Bassett, 2017). The immediate next step is to investigate whether there are coarse-grained shifts in brain-network topology during media use. Synchronization Theory predicts that flow corresponds to a stable network topology, which is distinct from the network topologies that emerge from a mismatch between task difficulty and individual ability. Accordingly, we should expect network stability within a given psychological state, but differences between psychological states. If the answer to these two questions is "yes," then the final (and rather risky) step will be to link

fine-grained changes in content to these brain dynamics. The capacity to test some of Sherry's (2004) predictions about how media content contribute to intensely-gratifying media experiences may finally be within reach.

Limitations

As with all studies, ours is not without limitation. There are two items worth considering. The first is related to network thresholding. The network measures used in this study required a sparse graph: that is, a graph where every node is not connected to every other node (Rubinov & Sporns, 2010). However, there is currently no convention for exactly how sparse a graph should be, although there is some reason to believe that nodes should not be disconnected (for an extended treatment of this issue, and its boundary conditions, see Fornito et al., 2016). The application of a stringent threshold (as we did in this study by keeping only the strongest 10% of connections) helps minimize the chance that spurious relationships are observed in the network (Fornito et al., 2016). But there is some concern that network results might differ by thresholding strategies. To test this, we applied several thresholds (i.e., 0.1, 0.2, 0.3, 0.4, 0.5; see Figure 2c) and observed similar results, regardless of strategy.

A second concern is related to null-network generation. Several different algorithms exist, each with different strengths and weaknesses (Fornito et al., 2016). As such, there is currently no gold-standard null network (for a detailed treatment of this issue, see Zalesky et al., 2012). Many of the emerging network neuroscience studies use the Maslov and Sneppen (2002) algorithm, which generates a random graph topology by shuffling edges between nodes while preserving the overall degree of each node in the network. However, since our study investigated the extent to which nodal degrees varied by condition, a null network algorithm that holds the degree invariant simply does not work. Accordingly, and following recommendations for generating null networks on fMRI data (Fornito et al., 2016; Zalesky et al., 2012), we applied the Hirschberger-Qi-Steuer algorithm. We did some testing to see whether our global efficiency results differed by null model selection, and did not observe differences. However, the Maslov and Sneppen algorithm is computationally costly, even on powerful computer clusters (Fornito et al., 2016). Therefore, extensive testing lies outside of the scope of the current study. Future research in this area might benefit from data-driven analyses to see whether different thresholding and null model decisions influence network characterization of the neural basis of flow. Similar work has already been done for dynamic analyses on brain networks (see e.g., Telesford et al., 2016).

Broader implications

Finally, these results suggest important updates to Synchronization Theory. First, the theory states that flow is an energetically-optimized state. This means that the performance to energy ratio is maximized during flow. One critique of the theory is that it was not very specific as to the basis of the comparison. Our results provide

this important insight by showing that flow is energetically optimized as compared to elevated connectivity in the DMN (commonly associated with tasks that are accomplished on autopilot) during both low-difficulty tasks and high-difficulty tasks that might be commonly associated with overload. A second point worth noting is related to the networked properties that underlie flow. While our results certainly implicate the networks specified by Synchronization Theory, they also suggest extensions. Our study evaluated network connectivity for 264 different ROIs, and observed high average degrees in memory and ventral attention networks during flow. This suggests new opportunities for theorizing, especially given that memory is so critical to cognitive control. Lastly, the present study applied global network measures to characterize brain network data. These represent a first start, but as our average degree analysis suggests, subgraphs within the network seem to vary by condition. This suggests that local network typologies may be worth exploring.

Future research should investigate local measures, in order to better understand the topological organization within and between brain networks during flow. This would allow for a more fine-grained understanding of issues related to local efficiency (e.g., Gu et al., 2018) and local reward processing (e.g., Duverne & Koechlin, 2017) during flow.

Conclusion

Here, we applied a network neruoscience approach to investigate the neural basis of flow during media use. Demonstrating the applicability of our approach, we are better able to test Synchronization Theory's H1 and provide a first-ever test of H3. More generally, graph theory offers a wealth of tools that are suitable for characterizing the brain during flow, such as the clustering coefficient of local networks, network motifs, and small-worldness, just to list a few (Rubinov & Sporns, 2010). Moreover, these approaches can be applied dynamically (Sizemore & Bassett, 2017), which allows for a better understanding of how flow emerges over time (a first-ever test of H2). Finally, if the these network properties truly characterize flow, then they should show a statistical relationship with self-reported flow (a test of H4).

The accumulation of this evidence will further validate neuromarkers of flow, which will assist in studying how content dynamics contribute to this highly-enjoyable psychological state. In the meantime, and answering calls for a more open science (e.g., Poldrack, 2012), we have made the data and code necessary to replicate and extend this study freely and openly available. Similarly, our stimulus (Asteroid Impact) is open-source and available for all to use and modify (we have also included the code necessary to replicate our experimental conditions). We hope that this encourages other labs to innovate and extend on these results, while mitigating the degree to which they must reinvent the wheel. The rapid accumulation of high-quality evidence in this area is critical to supporting or falsifying Synchronization Theory. We admit, this is truly an exciting time to be a communication scientist.

Supplementary material

Supplementary material are available at *Journal of Communication* online.

Acknowlegments

Notes

1 Given that there were 18 subjects, 4 runs, and 3 conditions per run, there should be a total of 216 correlation matrices. However, one run for one subject was removed due to an equipment malfunction, hence the total of 213 correlation matrices.
2 For more about this algorithm, see the Supplementary Appendix.
3 The formula for this calculation is provided in the Supplementary Appendix.
4 This calculation is formalized in the Supplementary Appendix.

References

Abraham, A., Pedregosa, F., Eickenberg, M., Gervais, P., Muller, A., Kossaifi, J., … Varoquaux, G. (2014). Machine learning for neuroimaging with scikit-learn. *Frontiers in Neuroinformatics, 8*(14), 1–10. doi:10.3389/fninf.2014.00014

Alakörkkö, T., Saarimäki, H., Glerean, E., Saramäki, J., & Korhonen, O. (2017). Effects of spatial smoothing on functional brain networks. *European Journal of Neuroscience, 46*(9), 2471–2480. doi:10.1111/ejn.13717

Andersson, J. L. R., Jenkinson, M., & Smith, S. M. (2007a). *Non-linear optimisation FMRIB technial report TR07JA1*. Oxford, England: FMRIB Centre.

Andersson, J. L. R., Jenkinson, M., & Smith, S. M. (2007b). *Non-linear registration aka spatial normalisation FMRIB technial report TR07JA2*. Oxford, England: FMRIB Centre.

Bassett, D. S., Bullmore, E. T., Meyer-Lindenberg, A., Apud, J. A., Weinberger, D. R., & Coppola, R. (2009). Cognitive fitness of cost-efficient brain functional networks. *Proceedings of the National Academy of Sciences, 106*(28), 11747–11752. doi:10.1073/pnas.0903641106

Bassett, D. S., & Gazzaniga, M. S. (2011). Understanding complexity in the human brain. *Trends in Cognitive Sciences, 15*(5), 200–209. doi:10.1016/j.tics.2011.03.006

Bassett, D. S., & Sporns, O. (2017). Network neuroscience. *Nature Neuroscience, 20*(3), 353–364. doi:10.1038/nn.4502

Berkman, E. T., & Falk, E. B. (2013). Beyond brain mapping: Using neural measures to predict real-world outcomes. *Current Directions in Psychological Science, 22*(1), 45–50. doi:10.1177/0963721412469394

Bullmore, E., & Sporns, O. (2012). The economy of brain network organization. *Nature Reviews Neuroscience, 13*(5), 336–349. doi:10.1038/nrn3214

Chen, H. (2006). Flow on the net-detecting Web users' positive affects and their flow states. *Computers in Human Behavior, 22*(2), 221–233. doi:10.1016/j.chb.2004.07.001

Cole, M. W., Pathak, S., & Schneider, W. (2010). Identifying the brain's most globally connected regions. *Neuroimage, 49*(4), 3132–3148. doi:10.1016/j.neuroimage.2009.11.001

Cole, M. W., Reynolds, J. R., Power, J. D., Repovs, G., Anticevic, A., & Braver, T. S. (2013). Multi-task connectivity reveals flexible hubs for adaptive task control. *Nature Neuroscience, 16*(9), 1348–1355. doi:10.1038/nn.3470

Cole, M. W., Yarkoni, T., Repovs, G., Anticevic, A., & Braver, T. S. (2012). Global connectivity of prefrontal cortex predicts cognitive control & intelligence. *Journal of Neuroscience, 32*(26), 8988–8999. doi:10.1523/JNEUROSCI.0536-12.2012

Csikszentmihalyi, M. (1975). *Beyond boredom and anxiety: The experience of play in work and games*. San Francisco, CA: Jossey-Bass, Inc.

Csikszentmihalyi, M. (1990). *Flow: The psychology of optimal experience*. New York, NY: HarperCollins Publishers.

Davison, E. N., Schlesinger, K. J., Bassett, D. S., Lynall, M.-E., Miller, M. B., Grafton, S. T., & Carlson, J. M. (2015). Brain network adaptability across task states. *PLoS Computational Biology, 11*(1), e1004029. doi:10.1371/journal.pcbi.1004029

Dixon, M. L., De La Vega, A., Mills, C., Andrews-Hanna, J., Spreng, R. N., Cole, M. W., & Christoff, K. (2018). Heterogeneity within the frontoparietal control network and its relationship to the default and dorsal attention networks. *Proceedings of the National Academy of Sciences of the United States of America, 115*(7), E1598–E1607. doi:10.1073/pnas.1715766115

Duverne, S., & Koechlin, E. (2017). Rewards and cognitive control in the human prefrontal cortex. *Cerebral Cortex, 27*(10), 5024–5039. doi:10.1093/cercor/bhx210

Falk, E. B., & Bassett, D. S. (2017). Brain and social networks: Fundamental building blocks of human experience. *Trends in Cognitive Sciences, 21*(9), 674–690. doi:10.1016/j.tics.2017.06.009

Falk, E. B., Cascio, C. N., & Coronel, J. C. (2015). Neural prediction of communication-relevant outcomes. *Communication Methods and Measures, 9*(1–2), 30–54. doi:10.1080/19312458.2014.999750

Fornito, A., Zalesky, A., & Bullmore, E. (2016). *Fundamentals of brain network analysis*. London, England: Academic Press.

Friston, K. J., Buechel, C., Fink, G. R., Morris, J., Rolls, E., & Dolan, R. J. (1997). Psychophysiological and modulatory interactions in neuroimaging. *Neuroimage, 6*(3), 218–229. doi:10.1006/nimg.1997.0291

Gilaie-Dotan, S. (2016). Visual motion serves but is not under the purview of the dorsal pathway. *Neuropsychologia, 89*, 378–392. doi:10.1016/j.neuropsychologia.2016.07.018

Goodale, M. A., & Milner, A. D. (1992). Separate visual pathways for perception and action. *Trends in Neurosciences, 15*(1), 20–25. doi:10.1016/0166-2236(92)90344-8

Greenwald, A. G. (2012). There is nothing so theoretical as a good method. *Perspectives on Psychological Science, 7*(2), 99–108. doi:10.1177/1745691611434210

Gu, S., Cieslak, M., Baird, B., Muldoon, S. F., Grafton, S. T., Pasqualetti, F., & Bassett, D. S. (2018). The energy landscape of neurophysiological activity implicit in brain network structure. *Scientific Reports, 8*(2057), 1–15. doi:10.1038/s41598-018-20123-8

Gu, S., Pasqualetti, F., Cieslak, M., Telesford, Q. K., Yu, A. B., Kahn, A. E., … Bassett, D. S. (2015). Controllability of structural brain networks. *Nature Communications, 6*(8414), 1–10. doi:10.1038/ncomms9414

Gyurkovics, M., Kotyuk, E., Katonai, E. R., Horvath, E. Z., Vereczkei, A., & Szekely, A. (2016). Individual differences in flow proneness are linked to a dopamine D2 receptor gene variant. *Consciousness and Cognition, 42*, 1–8. doi:10.1016/j.concog.2016.02.014

Hermundstad, A. M., Bassett, D. S., Brown, K. S., Aminoff, E. M., Clewett, D., Freeman, S., … Carlson, J. M. (2013). Structural foundations of resting-state and task-based functional connectivity in the human brain. *Proceedings of the National Academy of Sciences, 110*(15), 6169–6174. doi:10.1073/pnas.1219562110

Hirschberger, M., Qi, Y., & Steuer, R. E. (2007). Randomly generating portfolio-selection covariance matrices with specified distributional characteristics. *European Journal of Operational Research, 177*(3), 1610–1625. doi:10.1016/j.ejor.2005.10.014

Hosseini, S. M. H., Hoeft, F., & Kesler, S. R. (2012). Gat: A graph-theoretical analysis toolbox for analyzing between-group differences in large-scale structural and functional brain networks. *PLoS One, 7*(7), e40709. doi:10.1371/journal.pone.0040709

Huskey, R. (2016). Beyond blobology: Using psychophysiological interaction analyses to investigate the neural basis of human communication phenomena. In S. Kubitschko & A. Kaun (Eds.), *Innovative methods in media and communication research* (pp. 123–138). London, England: Palgrave Macmillan.

Huskey, R., Craighead, B., Miller, M. B., & Weber, R. (2018). Does intrinsic reward motivate cognitive control? A naturalistic-fMRI study based on the Synchronization Theory of Flow. *Cognitive, Affective, and Behavioral Neuroscience, 18*(5), 902–924. doi:10.3758/s13415-018-0612-6

Jenkinson, M., Bannister, P., Brady, M., & Smith, S. M. (2002). Improved optimization for the robust and accurate linear registration and motion correction of brain images. *Neuroimage, 17*(2), 825–841. doi:10.1006/nimg.2002.1132

Keller, J., & Bless, H. (2008). Flow and regulatory compatibility: An experimental approach to the flow model of intrinsic motivation. *Personality and Social Psychology Bulletin, 34*(2), 196–209. doi:10.1177/0146167207310026

Keller, J., & Blomann, F. (2008). Locus of control and the flow experience: An experimental analysis. *European Journal of Personality, 22*(1), 589–607. doi:10.1002/per.692

Klasen, M., Weber, R., Kircher, T. T. J., Mathiak, K. A., & Mathiak, K. (2012). Neural contributions to flow experience during video game playing. *Social Cognitive and Affective Neuroscience, 7*(4), 485–495. doi:10.1093/scan/nsr021

Kryston, K., Novotny, E., Schmälzle, R., & Tamborini, R. (2018). Social demand in video games and the snychronization thoery of flow. In N. D. Bowman (Ed.), *Video games: A medium that demands our attention* (pp. 161–177). New York, NY: Routledge.

Kueby, R., Larson, R., & Csikszentmihalyi, M. (1996). Experience sampling method applications to communication research questions. *Journal of Communication, 46*(2), 99–120. doi:10.1111/j.1460-2466.1996.tb01476.x

Lang, A., Bradley, S. D., Park, B., Shin, M., & Chung, Y. (2006). Parsing the resource pie: Using STRTs to measure attention to mediated messages. *Media Psychology, 8*(4), 369–394. doi:10.1207/s1532785xmep0804_3

Latora, V., & Marchiori, M. (2001). Efficient behavior of small-world networks. *Physical Review Letters, 87*(19), 198701. doi:10.1103/PhysRevLett.87.198701

Laufs, H., Kleinschmidt, A., Beyerle, A., Eger, E., Salek-Haddadi, A., Preibisch, C., & Krakow, K. (2003). EEG-correlated fMRI of human alpha activity. *Neuroimage, 19*(4), 1463–1476. doi:10.1016/S1053-8119(03)00286-6

Liu, S.-H., Liao, H.-L., & Pratt, J. (2008). Impact of media richness and flow on e-learning technology acceptance. *Computers and Education, 52*(1), 599–607. doi:10.1016/j.compedu.2008.11.002

de Manzano, Ö., Cervenka, S., Jucaite, A., Hellenäs, O., Farde, L., & Ullén, F. (2013). Individual differences in the proneness to have flow experiences are linked to dopamine D2-receptor availability in the dorsal striatum. *Neuroimage, 67*(15), 1–6. doi:10.1016/j.neuroimage.2012.10.072

Maslov, S., & Sneppen, K. (2002). Specificity and stability in topology of protein networks. *Science (New York, N.Y.), 296*(5569), 910–913. doi:10.1126/science.1065103

Mathiak, K. A., Klasen, M., Zvyagintsev, M., Weber, R., & Mathiak, K. (2013). Neural networks underlying affective states in a multimodal virtual environment: Contributions to boredom. *Frontiers in Human Neuroscience, 7*, 1–7. doi:10.3389/fnhum.2013.00820

Matthews, N. L. (2015). Too good to care: The effect of skill on hostility and aggression following violent video game play. *Computers in Human Behavior, 48*, 219–225. doi:10.1016/j.chb.2015.01.059

Monge, P., & Contractor, N. (2003). *Theories of communication networks*. New York, NY: Oxford University Press.

Mosing, M. A., Magnusson, P. K. E., Pedersen, N. L., Nakamura, J., Madison, G., & Ullén, F. (2012). Heritability of proneness for psychological flow experiences. *Personality and Individual Differences, 53*(5), 699–704. doi:10.1016/j.paid.2012.05.035

Mosing, M. A., Pedersen, N. L., Cesarini, D., Johannesson, M., Magnusson, P. K. E., Nakamura, J., … Ullén, F. (2012). Genetic and environmental influences on the relationship between flow proneness, locus of control and behavioral inhibition. *PLoS One, 7*(11), e47958. doi:10.1371/journal.pone.0047958

Nakamura, J., & Csikszentmihalyi, M. (2005). The concept of flow. In C. R. Snyder & S. J. Lopez (Eds.), *Handbook of positive psychology* (pp. 89–105). New York, NY: Oxford University Press.

Newman, M. E. J. (2010). *Networks: An introduction*. Oxford, England: Oxford University Press.

Nisbett, R. E., & Ross, L. (1980). *Human inference: Strategies and shortcomings of social judgment*. Englewood Cliffs, NJ: Prentice-Hall.

Novak, T. P., Hoffman, D. L., & Yung, Y.-F. (2000). Measuring the customer experience in online environments: A structural modeling approach. *Marketing Science, 19*(1), 22–42. doi:10.1287/mksc.19.1.22.15184

Oliver, M. B., Raney, A. A., Slater, M., Appel, M., Hartmann, T., Bartsch, A., … Das, H. H. J. (2018). Self-transcendent media experiences: Taking meaningful media to a higher level. *Journal of Communication, 68*(2), 380–389. doi:10.1093/joc/jqx020

Poldrack, R. A. (2012). The future of fMRI in cognitive neuroscience. *Neuroimage, 62*(2), 1216–1220. doi:10.1016/j.neuroimage.2011.08.007

Power, J. D., Cohen, A. L., Nelson, S. M., Wig, G. S., Barnes, K. A., Church, J. A., … Petersen, S. E. (2011). Functional network organization of the human brain. *Neuron, 72*(4), 665–678. doi:10.1016/j.neuron.2011.09.006

Pruim, R. H. R., Mennes, M., Buitelaar, J. K., & Beckmann, C. F. (2015). Evaluation of ICA-AROMA and alternative strategies for motion artifact removal in resting state fMRI. *Neuroimage, 112*, 278–287. doi:10.1016/j.neuroimage.2015.02.063

Pruim, R. H. R., Mennes, M., van Rooij, D., Llera, A., Buitelaar, J. K., & Beckmann, C. F. (2015). ICA-AROMA: A robust ICA-based strategy for removing motion artifacts from fMRI data. *Neuroimage, 112*, 267–277. doi:10.1016/j.neuroimage.2015.02.064

Raichle, M. E., MacLeod, A. M., Snyder, A. Z., Powers, W. J., Gusnard, D. A., & Shulman, G. L. (2001). A default mode of brain function. *Proceedings of the National Academy of Sciences, 98*(2), 676–682. doi:10.1073/pnas.98.2.676

Reinecke, L., & Oliver, M. B. (2017). Media use and well-being: Status quo and open questions. In L. Reinecke & M. B. Oliver (Eds.), *Handbook of media use and well-being: International perspectives on theory and research on positive media effects* (pp. 3–13). New York, NY: Routledge.

Risk, B. B., Kociuba, M. C., & Rowe, D. B. (2018). Impacts of simultaneous multislice acquisition on sensitivity and specificity in fMRI. *Neuroimage, 172*, 538–553. doi:10.1016/j.neuroimage.2018.01.078

Ross, S., & Keiser, H. (2014). Autotelic personality through a five-factor lens: Individual differences in flow-propensity. *Personality and Individual Differences, 59*(1), 3–8. doi:10.1016/j.paid.2013.09.029

Rubinov, M., & Sporns, O. (2010). Complex network measures of brain connectivity: Uses and interpretations. *Neuroimage, 52*(3), 1059–1069. doi:10.1016/j.neuroimage.2009.10.003

Sherry, J. (2004). Flow and media enjoyment. *Communication Theory, 14*(4), 328–347. doi:10.1111/j.1468-2885.2004.tb00318.x

Sizemore, A. E., & Bassett, D. S. (2017). Dynamic graph metrics: Tutorial, toolbox, and tale. *Neuroimage*. doi:10.1016/j.neuroimage.2017.06.081

Smith, S. M. (2002). Fast robust automated brain extraction. *Human Brain Mapping, 17*(3), 143–155. doi:10.1002/hbm.10062

Snijders, T. A. B., & Borgatti, S. P. (1999). Non-parametric standard errors and tests for network statistics. *Connections, 22*(2), 161–170.

Sporns, O. (2011). *Networks of the brain*. Cambridge, MA: The MIT Press.

Sporns, O. (2012). *Discovering the human connectome*. Cambridge, MA: The MIT Press.

Strogatz, S. (2003). *Sync: The emerging science of spontaneous order*. New York, NY: Hyperion.

Telesford, Q. K., Lynall, M.-E., Vettel, J., Miller, M. B., Grafton, S. T., & Bassett, D. S. (2016). Detection of functional brain network reconfiguration during task-driven cognitive states. *Neuroimage, 142*, 198–210.

Turner, B., Huskey, R., & Weber, R. (2018). Charting a future for fMRI in communication science. *Communication Methods and Measures*. doi:10.1080/19312458.2018.1520823

Ugurbil, K., Xu, J., Auerbach, E. J., Moeller, S., Vu, A. T., Duarte-Carvajalino, J. M., … Yacoub, E. (2013). Pushing spatial and temporal resolution for functional and diffusion MRI in the Human Connectome Project. *Neuroimage, 80*, 80–104. doi:10.1016/j.neuroimage.2013.05.012

Ulrich, M., Keller, J., & Grön, G. (2016a). Dorsal raphe nucleus down-regulates medial prefrontal cortex during experience of flow. *Frontiers in Behavioral Neuroscience, 10*, 1–9. doi:10.3389/fnbeh.2016.00169

Ulrich, M., Keller, J., & Grön, G. (2016b). Neural signatures of experimentally induced flow experiences identified in a typical fMRI block design with BOLD imaging. *Social Cognitive and Affective Neuroscience, 11*(3), 496–507. doi:10.1093/scan/nsv133

Ulrich, M., Keller, J., Hoenig, K., Waller, C., & Grön, G. (2013). Neural correlates of experimentally induced flow experiences. *Neuroimage, 86*(1), 194–202. doi:10.1016/j.neuroimage.2013.08.019

Vatansever, D., Menon, D. K., & Stamatakis, E. A. (2017). Default mode contributions to automated information processing. *Proceedings of the National Academy of Sciences, 114*(48), 12821–12826. doi:10.1073/pnas.1710521114

Weber, R., Alicea, B., Huskey, R., & Mathiak, K. (2018). Network dynamics of attention during a naturalistic behavioral paradigm. *Frontiers in Human Neuroscience, 12*(182), 1–14. doi:10.3389/fnhum.2018.00182

Weber, R., Fisher, J. T., Hopp, F. R., & Lonergan, C. (2017). Taking messages into the magnet: Method-theory synergy in communication neuroscience. *Communication Monographs, 85*(1), 81–102. doi:10.1080/03637751.2017.1395059

Weber, R., Huskey, R., & Craighead, B. (2017). Flow experiences and well-being: A media neuroscience perspective. In L. Reinecke & M. B. Oliver (Eds.), *Handbook of media use and well-being: International perspectives on theory and research on positive media effects* (pp. 183–196). New York, NY: Routledge.

Weber, R., Mangus, J. M., & Huskey, R. (2015). Brain imaging in communication research: A practical guide to understanding and evaluating fMRI studies. *Communication Methods and Measures, 9*(1–2), 5–29. doi:10.1080/19312458.2014.999754

Weber, R., Sherry, J., & Mathiak, K. (2008). The neurophysiological perspective in mass communication research: Theoretical rationale, methods, and applications. In M. J. Beatty, J. C. Mccroskey, & K. Floyd (Eds.), *Biological dimensions of communication: Perspectives, methods, and research* (pp. 41–71). Cresskill, NJ: Hampton Press.

Weber, R., Tamborini, R., Westcott-Baker, A., & Kantor, B. (2009). Theorizing flow and media enjoyment as cognitive synchronization of attentional and reward networks. *Communication Theory, 19*(4), 397–422. doi:10.1111/j.1468-2885.2009.01352.x

Weiss, S. A., Bassett, D. S., Rubinstein, D., Holroyd, T., Apud, J., Dickinson, D., & Coppola, R. (2011). Functional brain network characterization and adaptivity during task practice in healthy volunteers and people with schizophrenia. *Frontiers in Human Neuroscience, 5*, 1–14. doi:10.3389/fnhum.2011.00081

Wichers, M., Aguilera, M., Kenis, G., Krabbendam, L., Myin-Germeys, I., Jacobs, N., … van Os, J. (2008). The catechol-o-methyl transferase val158met polymorphism and experience of reward in the flow of daily life. *Neuropsychopharmacology: Official Publication of the American College of Neuropsychopharmacology, 33*(13), 3030–3036. doi:10.1038/sj.npp.1301520

Xia, M., Wang, J., & He, Y. (2013). BrainNet viewer: A network visualization tool for human brain connectomics. *PLoS One, 8*(7), e68910. doi:10.1371/journal.pone.0068910

Yarkoni, T., Poldrack, R. A., Nichols, T. E., Van Essen, D. C., & Wager, T. D. (2011). Large-scale automated synthesis of human functional neuroimaging data. *Nature Methods, 8*(8), 665–670. doi:10.1038/nmeth.1635

Zalesky, A., Fornito, A., & Bullmore, E. (2012). On the use of correlation as a measure of network connectivity. *Neuroimage, 60*(4), 2096–2106. doi:10.1016/j.neuroimage.2012.02.001

Appendix

HQS Algorithm

The Hirschberger-Qi-Steuer algorithm (HQS; Hirschberger et al., 2007) was used to generate null adjacency matrices based on empirically observed adjacency matrices; specifically, the unthresholded covariance matrix for a given experimental condition. The HQS algorithm generates a random covariance matrix by sampling a Gaussian distribution that is tuned based on the empirically observed covariance matrix. The HQS algorithm is shown in pseudo code in equation 1. For a given empirical covariance matrix, e is the mean and v is the variance of the off-diagonal and $\hat{e}$ is the mean of the diagonal.

$$
\begin{aligned}
&1.\ m \leftarrow max(2, \lfloor \hat{e}^2 - e^2/v \rfloor) \\
&2.\ \mu \leftarrow \sqrt{e/m} \\
&3.\ \sigma^2 \leftarrow -\mu^2 + \sqrt{\mu^4 + v/m} \\
&4.\ x_{i,j} \sim N(\mu, \sigma^2)\ i = 1, ..., N; j = 1, ..., m \\
&5.\ X = (x_{i,j})\ i = 1, ..., N; j = 1, ..., m \\
&6.\ C = X X^T
\end{aligned}
\tag{1}
$$

Global Efficiency

Global efficiency is the average of the inverse of the shortest path length for all nodes in a network (Latora & Marchiori, 2001). For binary undirected graphs (as we used in this study), this is formalized in equation 2, where N is the set of all nodes in a network, n is the number of nodes in the network, and d_{ij} is a the shortest path length between nodes i and j within N

$$
E = \frac{1}{n} \sum_{i \in N} E_i = \frac{1}{n} \sum_{i \in N} \frac{\sum_{j \in N j \neq i} d_{ij}^{-1}}{n - 1}
\tag{2}
$$

Inference Testing

Inference testing was conducted following a procedure for calculating paired-samples t-tests (two-tailed) as outlined by Snijders and Borgatti (1999). This is a modification of the classic paired samples t-test. The numerator of this equation remains unchanged in that it is the difference between two empirically observed network statistics. However, the denominator (which represents the standard error of the differences) is modified. In our case, the standard error of the differences is calculated based on the network statistic (i.e., global efficiency, average degree) observed in each null sparse graph rather than on the differences between two experimental conditions as observed in the sampling distribution (equation 3).

$$t = \frac{Z_1 - Z_2}{s.e._b} \tag{3}$$

Where Z_1 is the network statistic (i.e., average degree, global efficiency) for one condition (e.g., balanced-difficulty), Z_2 is the network statistic (i.e., average degree, global efficiency) for a second condition (e.g., high-difficulty), and where $s.e._b$ is represented by equation 4.

$$s.e._b = \sqrt{\frac{1}{M-1} \sum_{m=1}^{M} (Z^{*(m)} - Z^{*(.)})^2} \tag{4}$$

Where $Z^{*(m)}$ is the difference in the network statistic (i.e., average degree, global efficiency) between two randomly generated networks and $Z^{*(.)}$ is the mean difference in the network statistic (i.e., average degree, global efficiency) for all randomly generated networks, and M is the total number of random networks.